

Research Article

Comparison of Adsorption Capability of Activated Carbon and Metal Doped TiO₂ for Geosmin and 2-MIB Removal from Water

Aisha Asghar, Zahiruddin Khan, Nida Maqbool, Ishtiaq A. Qazi, and Muhammad Ali Awan

School of Civil and Environmental Engineering, Institute of Environmental Science and Engineering (IESE), National University of Science and Technology (NUST), Islamabad 44000, Pakistan

Correspondence should be addressed to Zahiruddin Khan; zahirkhan61@gmail.com

Received 11 August 2014; Accepted 11 October 2014

Academic Editor: Yuekun Lai

Copyright © 2015 Aisha Asghar et al. This is an open access article distributed under the Creative Commons Attribution License, which permits unrestricted use, distribution, and reproduction in any medium, provided the original work is properly cited.

This study stemmed from consumer complaints about earthy and musty off-flavours in treated water of Rawal Lake Filtration Plant. In recent years, several novel adsorbents have been developed from nanomaterials for enhancing the contaminant removal efficiency. This paper presents preparation and the use of new adsorbents Pt doped titania and Fe doped titania, for the adsorption capacity of Geosmin and 2-MIB from water under laboratory conditions and their comparison, with most widely used activated carbon, under batch and column experiments. Stock solutions were prepared by using Geosmin and 2-MIB standards, procured by Sigma Aldrich (England). Samples were analysed using SPME-GC-FID. The adsorption of Geosmin and 2-MIB on GAC conformed to the Freundlich isotherm, while that of adsorption on metal doped titania fit equally well to both Langmuir and Freundlich isotherms. Moreover, data, generated for the kinetic isotherm, confirmed that Geosmin and 2-MIB removal is a function of contact time. Breakthrough column tests using 125 mg/L Pt doped titania nanoparticles, coated on glass beads against 700 ng/L of off-flavours, attained later breakthrough and exhaustion points and removed 98% of Geosmin and 97% of 2-MIB at room temperature. All columns could be regenerated using 50 mL 0.1 molar sodium hydroxide.

1. Introduction

Supply of safe and aesthetically pleasing water, for human consumption, is essential for all treatment facilities. A common and recurrent problem in drinking water is the formation of earthy-musty taste and odor [1]. Taste and odor episodes in drinking water are the cause for most consumer complaints [2]. There is growing concern about off-flavour in Rawal Lake Filtration Plant, which intensifies in summer months [3–5]. Sensory analysis detected earthy and musty off-flavours in raw, as well as in treated supplies from this facility. This study focused on Geosmin (C₁₂H₂₂O) and 2-MIB (C₁₁H₂₀O) as surrogate for earthy and musty off-flavours. Earthy and musty off-flavours are produced as secondary metabolite by two groups of aquatic microorganism: (i) *anabaena* for Geosmin and (ii) *Phormidium* spp. for 2-MIB [6]. Both compounds are semivolatile, saturated tertiary alcohols that can be detected at extremely low concentrations of 6–20 ng/L [7]. The main problem with the presence

of Geosmin/2-MIB is that conventional water treatment processes including coagulation, flocculation, and filtration are inadequate for their removal [8]. Oxidants including KMnO₄, ozonation, and UV/H₂O₂ have been tested for removal of odorous compounds [9, 10] but due to the complex tertiary structures of Geosmin and 2-MIB, these are resistant toward oxidation and most aquatic oxidants [11]. Activated carbon in combination with sand media in filtration plants is considered as one of the best available practice for the removal of off-flavours from water, but at relatively higher amount of pollutant levels, its adsorption efficiency drops [12–14]. Literature review reveals that nanoparticles have some advantages in using adsorption processes to solve many environmental issues due to their unique surface and structural properties [15]. A number of studies have been reported on photo catalysis of Geosmin and 2-MIB [16]; however, to the best of our knowledge no previous study has been reported on adsorption of Geosmin and 2-MIB using

TABLE 1: Method of metal doped-Titania nanoparticles preparation.

| Type of doping | Doped element | Method of preparation |
|----------------|---------------|---|
| Metal doping | Pt | 150 mL deionized water + 25 gm. titania + 1 molar ratio PtCl_4 |
| | | Stirred at 250 rpm for 24 hours |
| | Fe | Suspensions removed and oven dried at 110°C |
| | | Calcinated at 400°C for 6 hours, grounded, and stored in dark |
| | | 150 mL deionized water + 25 gm titania + 1.5 molar ratio FeCl_2 |
| | | Stirred at 250 rpm for 24 hours |
| | | Suspensions removed and oven dried at 100°C |
| | | Calcinated at 350°C for 8 hours, grounded, and stored in dark |

metal doped titania nanoparticles. Since metal doping further enhances the adsorption efficiency of nanoparticles [17, 18], this study aimed at comparing activated carbon, Fe-TiO₂, and Pt-TiO₂ nanoparticles for Geosmin/2-MIB removal, using breakthrough column studies, from synthetic and Rawal Lake Filtration Plant (RLFP), Pakistan, treated water samples.

2. Materials and Methods

2.1. Material Systems. The GC standard of Geosmin and 2-MIB were purchased from Sigma-Aldrich (Germany) at a concentration of 2 mg/L and 10 mg/L in methanol, respectively. Stock solutions were prepared in 10 mL methanol. General purpose reagent titanium (IV) oxide (Riedel-De Haen) was used as a source of titania nanoparticles; ferrous chloride and platinum chloride were purchased from Merck, Germany. Other chemicals including GC grade methanol, dichloromethane (DCM), and wood based granular and powdered activated carbon (Norit CIA) were procured from Acros, Organics, USA.

3. Experimentation

3.1. Synthesis of Nanoparticles. Liquid impregnation method was used to prepare metal doped titania nanoparticles [19] as described in Table 1.

3.2. Scanning Electron Microscopy of Adsorbents. SEM images were measured using JEOL JSM 6460 scanning electron microscope. Microscope operated at an acceleration voltage of 5, 10, and 15 kV and filament current of 60 mA. SEM was performed to find the surface morphology, topography, microstructure, and composition of adsorbents. The porous texture characterization of the samples was obtained by physical adsorption of gases. From N₂ adsorption data at -196°C (Autosorb-6B apparatus from Quantachrome [20]) the specific BET surface area (S_{BET}) was determined by applying the Brunauer-Emmett-Teller (BET) equation.

3.3. Analytical Method. Geosmin and 2-MIB were analysed using solid phase microextraction coupled with gas

chromatograph-flame ionized detector (SPME-GC-FID). One gram of sodium chloride was placed in a 15 mL vial containing 3 mL of the aqueous sample. The vial was sealed with Teflon-lined septum. The samples were heated to 65°C , and the SPME fiber (divinylbenzene-carboxen-polydimethylsiloxane SPME fiber) was inserted into heads space for 15 min equilibrium adsorption period. The fiber was then withdrawn from the sample and injected into the injection port of Shimadzu 2010 series Gas Chromatograph coupled with FID. The column used was fused silica capillary column with a length of 30 m, inner diameter of 0.32 mm, and wall thickness of $0.5\ \mu\text{m}$. The column temperature was set at 60°C for 1 min and then raised to 160°C @ $15^\circ\text{C}/\text{min}$, held at 160°C for 1 min, then raised to 200°C @ $10^\circ\text{C}/\text{min}$, again held at 200°C for 1 min, and finally temperature was raised to 260°C and held constant for 1 min. Total program time was 16.67 min. Detector temperature was 280°C while injector was set at 300°C . Split ratio was zero. Nitrogen was the makeup gas and Helium was used as carrier gas. Total flow rate was 6.6 mL/min. The extracts were stable and could be stored for up to two months with no apparent loss of analytes and concentrations as low as 1 ng/L could be detected.

3.4. Synthetic Solutions Preparation. Geosmin and 2-MIB solutions used in this study were prepared in the laboratory by dissolving stock solutions in ultrapure water. This study was aimed at testing adsorbents for their ability to adsorb earthy-musty odorants for the concentrations which are present in lake water. For this reason, sampling was performed from Rawal Lake Filtration Plant (RLFP) in the month of July, when taste and odor episode in treated water was at their maximum levels. RLFP draws raw water from Rawal Lake, Pakistan. Its treatment processes include coagulation, flocculation, sedimentation, sand filtration, and disinfection, which were inadequate to remove taste and odor from water. Average concentration of Geosmin and 2-MIB in treated water samples was 690 ng/L and 678 ng/L, respectively; hence, synthetic solution with 700 ng/L of odorants was prepared for batch adsorption and column adsorption experiments. All reactors were wrapped with aluminium foil during nanoparticle experiments, to restrict photo catalytic activity and to ensure adsorption as the only mechanism of odorant removal.

3.5. Batch Experiments

3.5.1. Adsorption Conditions Optimization. In this study, adsorbent dose, contact time, and stirring rate per minute for Geosmin and 2-MIB were optimized. For optimization of adsorbent dose for Geosmin and 2-MIB removal, adsorption experiments were performed by varying adsorbents doses between 40 mg/L and 200 mg/L in test solutions, containing 700 ng/L initial odorants concentration. In order to determine the equilibrium adsorption time, flasks containing 700 ng/L initial Geosmin and 2-MIB concentrations with optimized adsorbent dose were agitated on the orbital shaker for different time intervals (5, 15, 30, 45, 60, 75, 90, and 120 minutes). Similarly, test solutions were tested for the

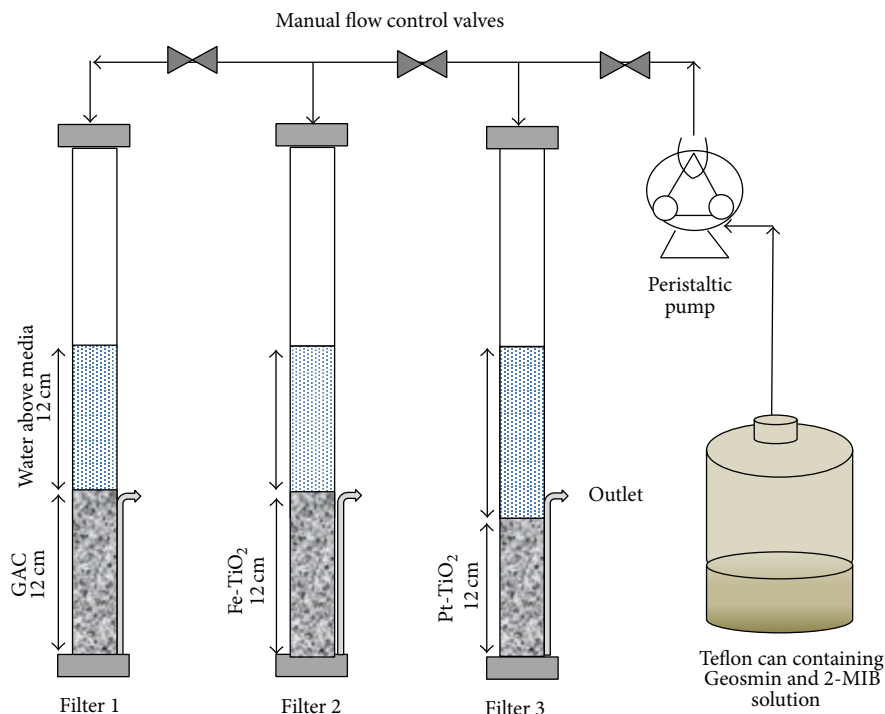


FIGURE 1: Schematics of the pilot column setup.

best stirring rate (between 25 and 200 rpm), with optimised adsorbent doses and contact time.

3.5.2. Removal Efficiency Calculation. To determine the removal efficiency of selected adsorbents, 100 mL of test solution with initial off-flavours concentration of 700 ng/L was taken in 250 mL conical flask at room temperature. 125 mg of the adsorbents (GAC, Fe, and Pt doped nanoparticles) were added in each test solution and stirred at orbital shaker at 100 rpm for one hour. All the samples were stored in dark brown vials, till final concentration analysis. Samples were subjected to filtration through prewashed 0.45 μm filters, to remove any solid adsorbents residue, prior to the gas chromatographic analysis.

Amount of Geosmin and 2-MIB adsorbed (ng/g) was calculated using [21]

$$q_e = \frac{(C_i - C_s)V}{m}, \quad (1)$$

where C_i is the initial analyte concentration, C_s is the residual equilibrium analyte concentrations (ng/L), V is the volume of the solution (mL), and m is the mass of adsorbent (mg) used in test solution.

3.5.3. Adsorption Isotherm Studies. For adsorption studies, 100 mL of the initial test solution of odorant concentrations, varying between 200 and 1200 ng/L, was taken in 1000 mL volumetric flasks and experiments were performed with all optimized conditions. 125 mg metal doped nanoparticles and 160 mg GAC were added to the test solutions and then placed

on an orbital shaker at 100 rpm for 60 minutes and final concentrations were determined, in all removal experiments.

3.5.4. Kinetic Studies. Several models are available to express the mechanism of adsorption of solute onto the adsorbent. For kinetic studies, 500 mg of adsorbent doses was introduced into 1000 mL solutions with initial analytes concentration of 700 ng/L and placed at an orbital shaker at a rotation speed of 100 rpm. Samples were taken at predetermined intervals up to 120 min. The kinetic analysis was carried out at room temperature ($25 \pm 1^\circ\text{C}$).

3.6. Pilot Scale Column Experiments. These experiments were designed to investigate efficiency of granular activated carbon and metal doped titania nanoparticles in fixed bed columns. Column design was based on study by Tang et al. [19]. Pilot setup consisted of three glass columns each having internal diameter 1.5 cm and empty bed contact time was 10.5 min. Media depth for all columns was 12 cm. Column one is comprised of granular activated carbon having 0.56 mm mean particle size. Other two columns were filled by glass beads coated with Fe and Pt doped titania nanoparticles. Each column had glass wool at their base, as the supporting media. Flowrate through these columns was controlled using a peristaltic pump attached to the three-way manifold. 700 ng/L Geosmin and 2-MIB solutions were passed through these columns at 2 mL/min. Figure 1 shows schematic of the pilot column setup.

3.6.1. Glass Beads Etching and Coating. Nanoparticles coated glass beads were used in filter columns. Sterilized glass beads

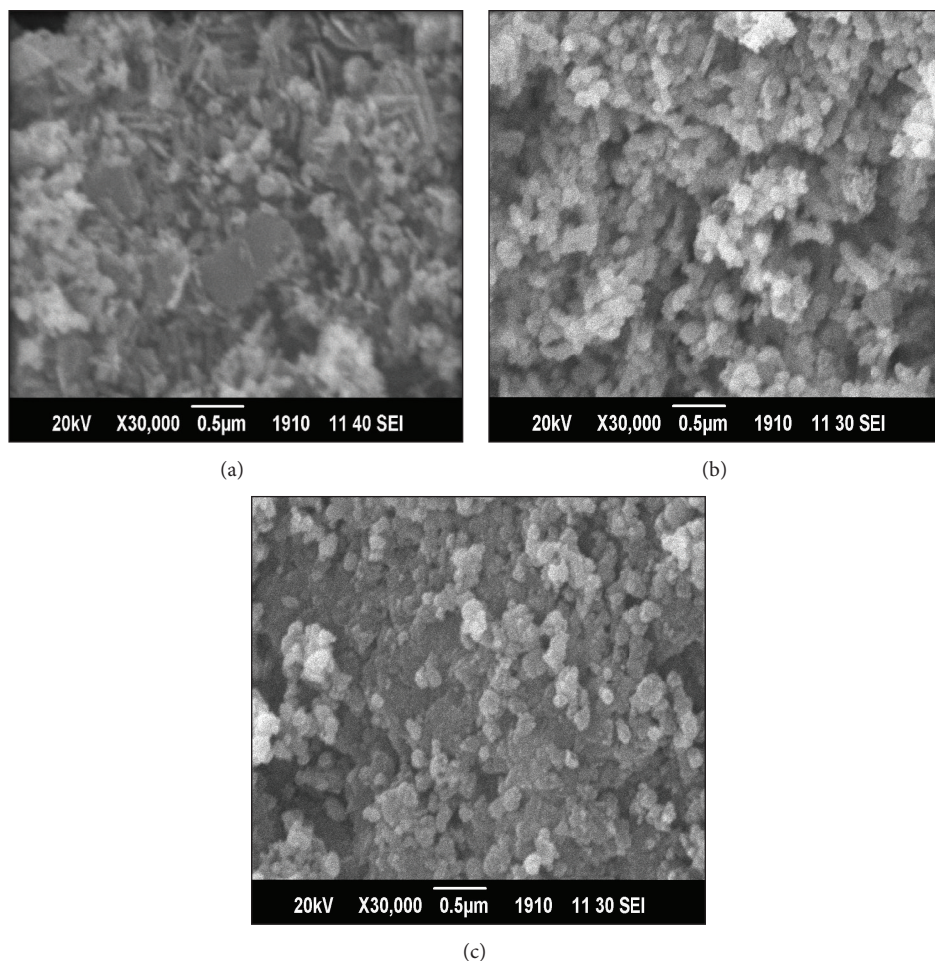


FIGURE 2: SEM micrograph of adsorbents at 30,000 resolution: (a) granular activated carbon and (b) Fe-TiO₂ (c) Pt-TiO₂ nanoparticles.

were dipped in 10% hydrogen fluoride solution and covered for 24 hours. Next, glass beads were stirred with metal doped titania nanoparticles aqueous solution, at 250 rpm for half an hour. After oven drying at 110 °C for 20 min these coated beads were shifted to furnace at 400 °C. Finally these were washed with distilled water, dried, and stored in dark.

3.6.2. Breakthrough Curves. Removal efficiency of the adsorption columns was represented by “break through curves” drawn from results, which showed that the concentration ratios (C/C_o) were a function of throughput volumes. Keeping in view the very low concentration of the pollutants, the breakthrough time and exhaustion time were set as $C/C_o = 0.02$ and $C/C_o = 0.95$, respectively. Samples for residual Geosmin and 2-MIB analysis were drawn after 10 bed volumes.

3.6.3. Column Desorption Study. In this study, after exhaustion of column, desorption study was carried out by pouring 50 mL of 0.1 M NaOH solution as an eluent, which was known to be efficient for column recovery [22]. Moreover, the adsorbent column was washed with distilled water before the next adsorption-desorption cycles. The adsorption-desorption

cycles were repeated thrice using the optimized condition to check the sustainability of the column for repeated use.

3.7. Geosmin and 2-MIB Removal from Rawal Lake Filtration Plant Water. Adsorption capacity of the abovementioned adsorbents was tested to remove Geosmin and 2-MIB from natural water samples collected from Rawal filtration plant in batch and column experiments under optimized adsorption conditions.

4. Results and Discussion

4.1. Characterisation of Adsorbents. For the direct examination of particle size and surface morphology of the samples SEM was used. All the particles were spheroid or oblate spheroid loosed and macropores can be clearly seen in the SEM micrographs. Scans of nanoparticles at $\times 30,000$ resolution are represented in Figure 2. The crystalline sizes of the adsorbents were in the range of 24 to 51 nm (activated carbon (43.5 nm), Fe-TiO₂ (38.5 nm), and Pt-TiO₂ (41.6 nm)). SEM images of Fe-TiO₂ and Pt-TiO₂ nanoparticles confirmed the presence of more porous, sponge-like structure of high roughness and complexity, as compared to activated carbon,

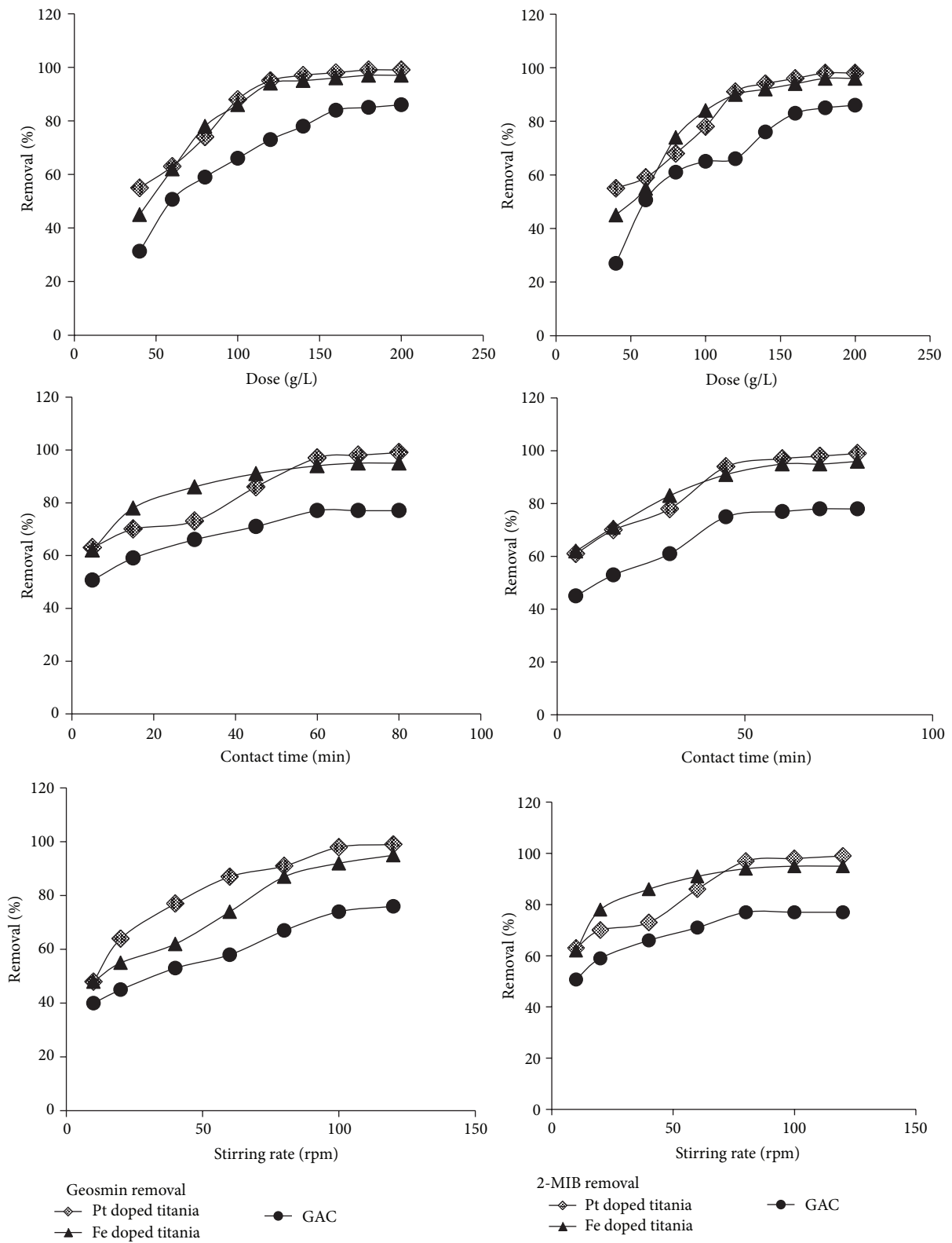


FIGURE 3: Dose, contact time, and stirring rate optimization for adsorbents.

TABLE 2: Removal efficiency of adsorbents used.

| Adsorbents | GAC | | Fe-TiO ₂ | | Pt-TiO ₂ | |
|------------|---------|-------|---------------------|-------|---------------------|-------|
| | Geosmin | 2-MIB | Geosmin | 2-MIB | Geosmin | 2-MIB |
| % removal | 82 | 76 | 96 | 94 | 99 | 98 |

TABLE 3: Freundlich constant parameters for Geosmin and 2-MIB analysis.

| Adsorbate | Adsorbent | Freundlich isotherm parameters | | |
|-----------|---------------------|--------------------------------|------|-------|
| | | k_f | n | R^2 |
| 2-MIB | GAC | 0.64 | 3.12 | 0.97 |
| | Fe-TiO ₂ | 0.70 | 3.70 | 0.98 |
| | Pt-TiO ₂ | 0.71 | 4.00 | 0.99 |
| Geosmin | GAC | 0.65 | 3.10 | 0.97 |
| | Fe-TiO ₂ | 0.71 | 4.18 | 0.98 |
| | Pt-TiO ₂ | 0.86 | 4.38 | 0.99 |

TABLE 4: Langmuir constant parameters for Geosmin and 2-MIB analysis.

| Adsorbate | Adsorbent | Langmuir isotherm parameters | | | |
|-----------|---------------------|------------------------------|------|-------|-------|
| | | V_m | K | R_L | R^2 |
| 2-MIB | GAC | 0.62 | 0.80 | 0.71 | 0.98 |
| | Fe-TiO ₂ | 0.64 | 1.14 | 0.58 | 0.99 |
| | Pt-TiO ₂ | 0.70 | 1.56 | 0.56 | 0.99 |
| Geosmin | GAC | 0.64 | 0.90 | 0.69 | 0.98 |
| | Fe-TiO ₂ | 0.70 | 1.35 | 0.60 | 0.99 |
| | Pt-TiO ₂ | 0.72 | 1.53 | 0.57 | 0.99 |

Value of R_L interpretation: greater than 1 indicates unfavourable isotherm, equal to 1 means linear isotherm, between 0-1 shows favourable isotherm, and 0 indicates irreversible isotherm.

indicating the high surface area for adsorption. BET surface areas for three adsorbents tested were 567 m²/g, 423 m²/g, and 274 m²/g for Pt-TiO₂, Fe-TiO₂, and activated carbon, respectively.

4.2. Adsorption Conditions Optimization. Adsorption condition optimization results are demonstrated in Figure 3. The batch adsorption experiments were carried out by using various amounts adsorbent types.

Similar removal trends were observed for both Geosmin and 2-MIB removal, with increasing adsorbent doses. It was observed that, even on increasing the amount of adsorbent doses in the solution, the percentage removal of Geosmin and 2-MIB increased gradually and % removal plateaued at 125 mg/L for metal doped nanoparticles while 160 mg/L was found to be optimized GAC dosage. Adsorption capacities of the three adsorbent types at different contact times, when all other variables are constant, were determined. The maximum adsorption capacity of Geosmin and 2-MIB was obtained within contact time of 60 min, with optimized adsorbents dosage for all adsorbents studied. After optimizing PAC dosage and contact time final experiments were performed to

explore optimum mixing rate. Results illustrate that stirring rate had remarkable effects on rate of adsorption as with the increase in speed contact between adsorbent and adsorbate increases. Maximum adsorption of Geosmin and 2-MIB was observed at mixing rate of 100 rpm using optimized adsorbent doses, within a contact time of 60 min.

4.3. Removal Efficiency of Adsorbents. Removal efficiencies of the selected adsorbents are given in Table 2. Results indicate that removal efficiencies of metal doped titania particles were much higher, as compared to Granular activated carbon. Overall, Pt doped titania nanoparticles showed the best removal efficiency towards Geosmin and 2-MIB.

4.4. Adsorption Isotherms. Removal efficiencies of adsorbents were tested through isotherm studies. The linear form of the isotherm studies helped in better understanding of the adsorption phenomena. Freundlich and Langmuir equation explained adsorption of Geosmin and 2-MIB on different adsorbent concentrations, as discussed in the next sections.

Freundlich equation was used in this study as given below [23]

$$\log q_e = \log K + \frac{1}{n} \log C_e, \quad (2)$$

where q_e = equilibrium loading of Geosmin and 2-MIB on the GAC (ng/mg), C_e = equilibrium concentration of Geosmin and 2-MIB in the water (ng/L), k_f = adsorption capacity at unit concentration (ng/mg), $1/n$ = heterogeneity of adsorbent, and $1/n$ and k_f were obtained from slope and intercept of linear plot between $\log q_e$ and $\log C_e$.

From data stated in Table 3, it is clear that the Freundlich model is statistically valid for all adsorbents analyzed. To compare different adsorbents, usually the adsorbent with the higher amount of adsorbate adsorbed, at the desired effluent concentration, is preferred for the particular application. A number of carbon physical and chemical properties affect adsorption toward a particular adsorbate. For Geosmin and 2-MIB, the hydrophobic compounds, the amount of surface area associated with the adsorbate is critically important. The Freundlich constants (n and k) given in Table 3 for each adsorbent and the resulting curves are shown in Figure 4. The values of Freundlich constant K_{ef} indicate that this model gives a good fit to both Geosmin and 2-MIB. Values of constants were highest for Pt doped titania nanoparticles showing great affinity of the binding sites of adsorbent towards both adsorbates with the values 0.86 and 0.71 for Geosmin and 2-MIB, respectively. In contrast, the K_f values for GAC for removal of adsorbates are lowest, showing lowest adsorption ability of GAC among all adsorbents compared.

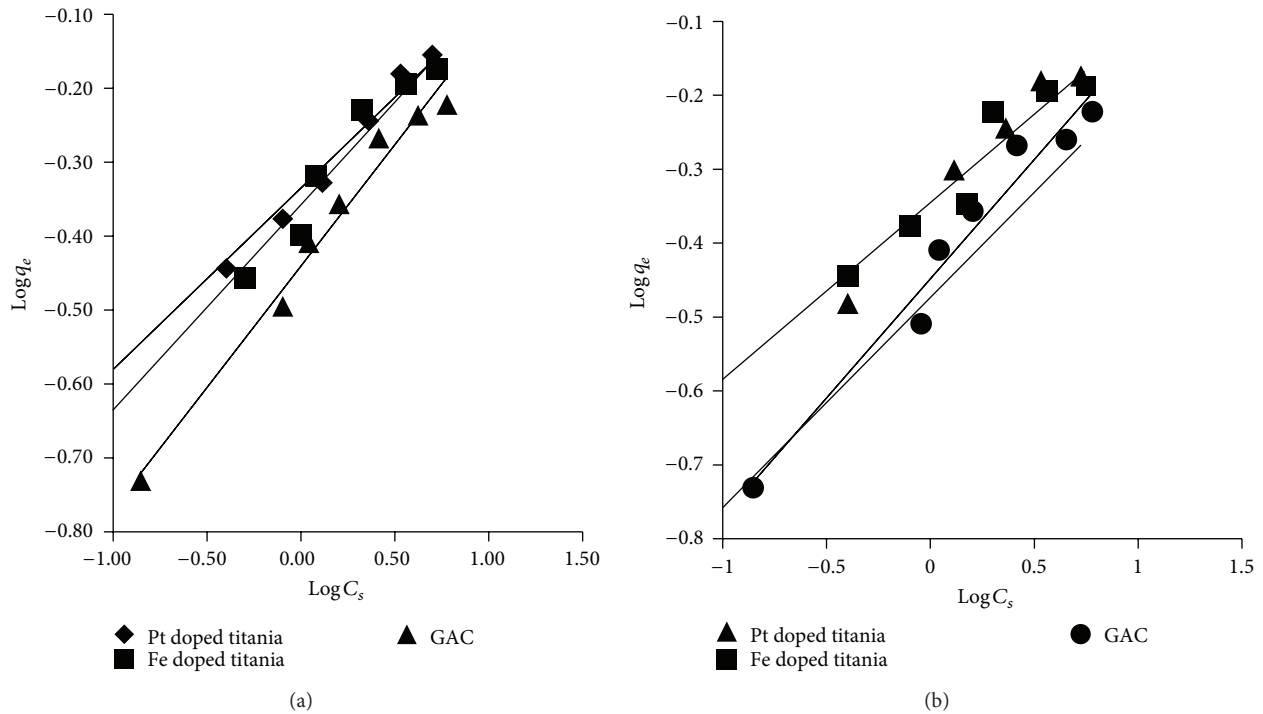


FIGURE 4: (a) Freundlich isotherms curve for adsorption of Geosmin at $18 \pm 2^\circ\text{C}$. (b) Freundlich isotherms curve for adsorption of 2-MIB at $18 \pm 2^\circ\text{C}$.

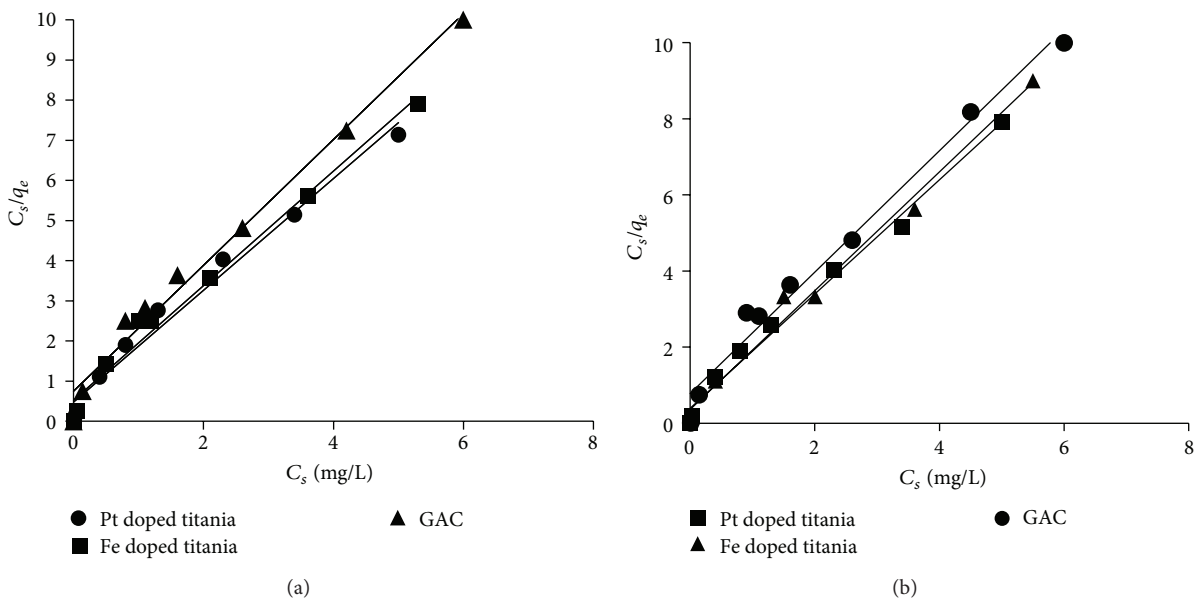


FIGURE 5: (a) Langmuir isotherm curve for adsorption of Geosmin at $18 \pm 2^\circ\text{C}$. (b) Langmuir isotherm curve for adsorption of 2-MIB at $18 \pm 2^\circ\text{C}$.

Mathematical form of Langmuir isotherm is given below [24]

$$\frac{C_e}{q_e} = \frac{C_e}{V_m} + \frac{1}{KV_m}, \quad (3)$$

where q_e = equilibrium loading of Geosmin and 2-MIB on the GAC (ng/mg), C_e = equilibrium concentration in the water

(ng/L), and V_m = maximum adsorption capacity (ng/mg). Values of K and V_m were obtained directly from intercept and slope of linear plot between C_s/q_e and C_s . Langmuir constants are described in Table 4.

Langmuir isotherms curves for Geosmin and 2-MIB are shown in Figure 5. Values for adsorption coefficient K and monolayer capacity V_m are higher for Pt doped

TABLE 5: Pseudo-second order parameters for Geosmin for and 2-MIB analysis.

| Adsorbate | Adsorbent | q_e (mg/g) | Pseudo-second-order equation parameters | | |
|-----------|---------------------|--------------|---|----------------|-------|
| | | | k (g/mg min) | h (mg/g min) | R^2 |
| 2-MIB | GAC | 0.39 | 0.98 | 0.12 | 0.99 |
| | Fe-TiO ₂ | 0.58 | 1.02 | 0.24 | 0.99 |
| | Pt-TiO ₂ | 0.61 | 1.10 | 0.35 | 0.99 |
| Geosmin | GAC | 0.43 | 0.14 | 0.15 | 0.99 |
| | Fe-TiO ₂ | 0.62 | 0.09 | 0.23 | 0.98 |
| | Pt-TiO ₂ | 0.67 | 1.04 | 0.37 | 0.99 |

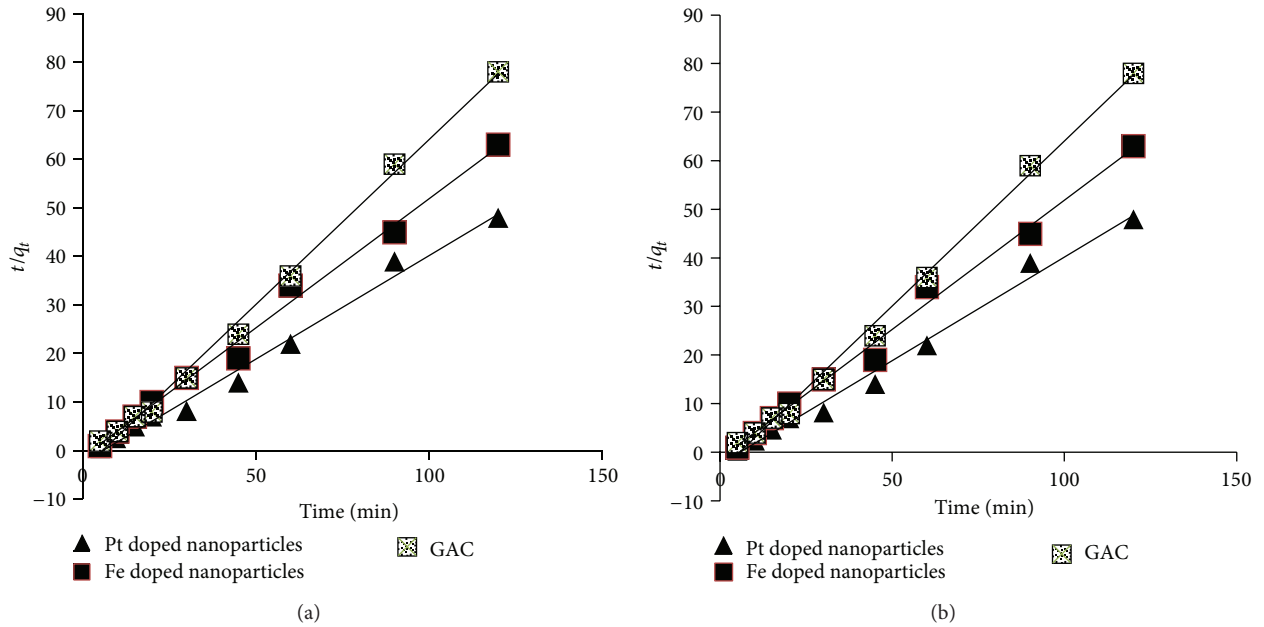
FIGURE 6: (a) Pseudo-second-order kinetic models for 2-MIB at $18 \pm 2^\circ\text{C}$. (b) Pseudo-second-order kinetics model for Geosmin at $18 \pm 2^\circ\text{C}$.

TABLE 6: Water quality parameters of RLFP treated water.

| Quality parameter | Range | Units |
|-------------------|-----------|------------------|
| DOC | 3.3–5.4 | mg/L |
| Turbidity | 0.1–0.2 | NTU |
| pH | 6.5–7 | — |
| Conductivity | 500–700 | S/cm |
| NOM | 3.35–5.5 | mg/L |
| UV ₂₅₄ | 0.05–0.90 | cm ⁻¹ |
| Geosmin | 690 | ng/L |
| 2-MIB | 657 | ng/L |

tania nanoparticles. These results explicitly indicate more favourable adsorption of Geosmin and 2-MIB on metal doped titania nanoparticles as compared to GAC.

The shape of the isotherm can be used to examine the favourability of the adsorbent. It was done by another dimensionless quantity, R_L , given by the following equation:

$$R_L = \frac{1}{1 + (KC_0)}, \quad (4)$$

where R_L is the dimensionless separation factor, C_0 is the initial Geosmin and 2-MIB concentrations, and K is the Langmuir constant. R_L values ranged between 0.69 and 0.57 for Geosmin and 0.71–0.56 for 2-MIB. It showed favourable isotherms for both off-flavours. Values for both isotherm constants are higher in case of Geosmin which clearly suggest preferred adsorption of Geosmin on all adsorbents, compared to 2-MIB. Cook et al., 2004, also reported that Geosmin showed better adsorption than 2-MIB on activated carbon and this was attributed to the lower molecular weight and higher solubility of Geosmin [25].

4.5. Kinetic Isotherms. A pseudo-second-order model (5) was used to describe the kinetics of adsorption [26]:

$$\frac{dq_t}{dt} = k(q_e - q_t)^2, \quad (5)$$

where q_t is the adsorption capacity (mg/g) at any time interval, q_e is the adsorption capacity (mg/g) at the equilibrium, and k (g mg⁻¹ min⁻¹) is the pseudo-second-order rate constant.

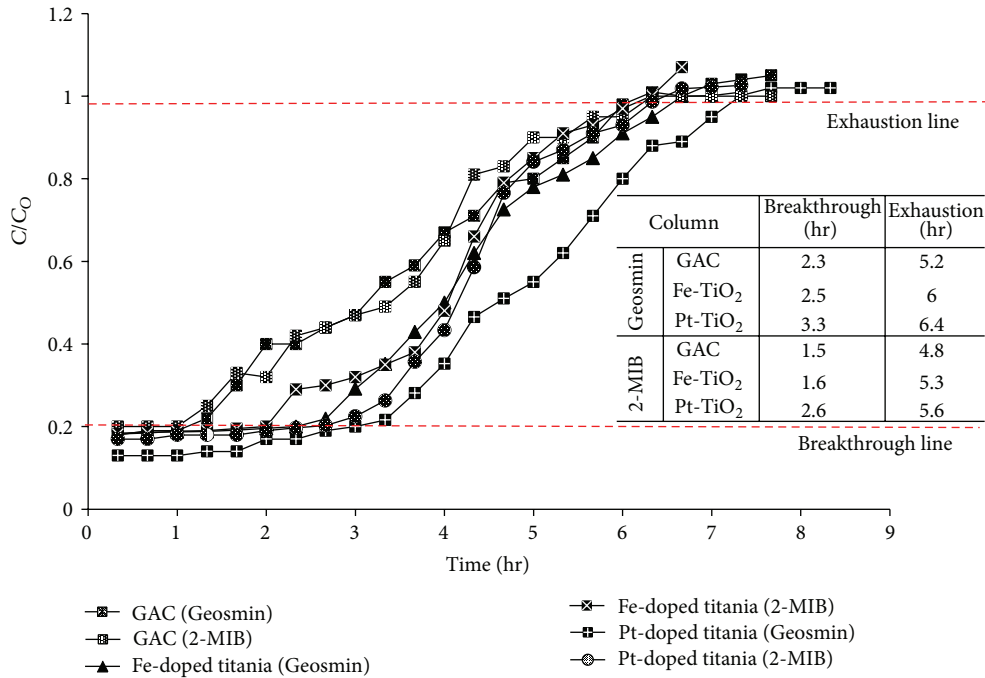


FIGURE 7: Breakthrough curves for Geosmin and 2-MIB at 18 ± 2 °C.

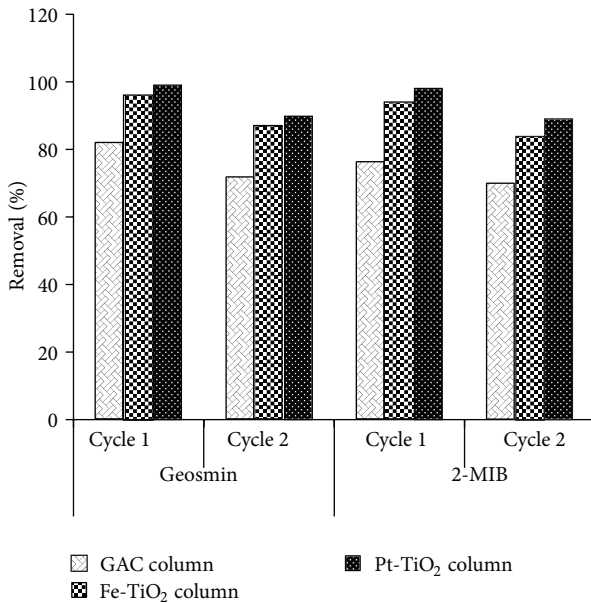


FIGURE 8: Adsorption capacities for columns after regeneration.

Integrating (5) with the following boundary conditions: $t = 0$ to t and $q_t = 0$ to q_t , gives

$$\frac{1}{q_e - q_t} = \frac{1}{q_e} + kt. \tag{6}$$

Equation (6) can be linearized as follows:

$$\frac{t}{q_t} = \frac{1}{kq_e^2} + \frac{1}{q_e}t. \tag{7}$$

Thus, the parameters k and q_e can be obtained from the intercept and slope of the plot of (t/q_t) against t .

The kinetic data obtained from batch adsorption tests was analyzed by using the pseudo-second-order model. Figure 6 shows the linearized plots of the results. The kinetics of Geosmin and 2-MIB adsorption were studied in batch adsorption tests, with three different adsorbents. Results clearly indicate that the removal efficiency is a function of contact time; moreover, maximal q_e and k values were obtained with Pt doped nanoparticles. All pseudo-second-order parameters are listed in Table 5. The data demonstrate a good compliance with the pseudo-second-order equation, as the regression coefficients for the linear plots were higher than 0.98 for all the adsorbents tested.

4.6. Column Experiments Results. Column efficiencies were determined in terms of breakthrough and column exhaustion times. At the beginning, removal through columns was very efficient as the adsorbents were fresh with all of their adsorption sites available. With the passage of time, some of the adsorption sites got exhausted and effluent concentrations started rising. After all the adsorption sites were exhausted, the inlet and the outlet concentrations became nearly the same. Column 1 having granular activated carbon was not found very effective either for Geosmin or 2-MIB. It attained early breakthrough and exhaustion points. Figure 7 illustrates breakthrough curves, breakthrough points, and exhaustion points for Geosmin and 2-MIB, respectively.

Overall comparison of adsorbents indicated that Pt-doped titania nanoparticles were most efficient for Geosmin and 2-MIB removal. Geosmin removal was a bit higher than 2-MIB in this case as well.

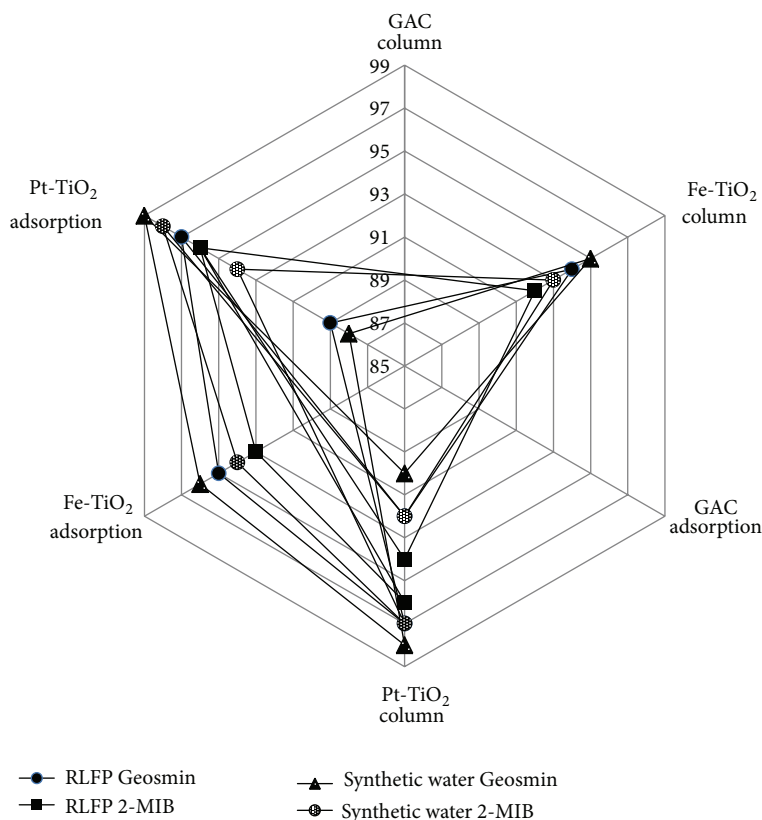


FIGURE 9: Comparison of Geosmin and 2-MIB removal from synthetic and RLFP water samples.

4.7. Column Desorption. For a viable sorption process, columns desorption and regeneration are important. The exhausted 12 cm bed volume columns (for all the three types of columns) were successfully regenerated using 0.1M of NaOH solution. The results (Figure 8) show that, on average, the columns could be used again by losing only 8% of their adsorption ability in successive cycle.

4.8. Geosmin and 2-MIB Removal Using RLFP Treated Water. The above-stated experiments were performed using synthetic solution of Geosmin and 2-MIB. Finally, experiments were conducted with the RLFP treated water samples. Average concentration of Geosmin and 2-MIB in composite water samples was 690 ng/L and 678 ng/L, respectively. Water quality data for water from RLFP is given in Table 6.

A comparison of taste and odor removal efficiency using adsorption and Column tests is presented in Figure 9. According to the results better removal was achieved with synthetic water as compared to the sample of treated water from RLFP. This difference can be attributed to organic matter and several interfering species in the treated water samples (Table 6). High removal efficiencies of 97–99% for Geosmin and 96–98% for 2-MIB from both synthetic and treated water samples confirm effectiveness of metal doped nanoparticles.

5. Conclusions

The present experimental results suggest that metal doped titania nanoparticles demonstrate significant adsorption

potential for the accelerated removal for earthy-musty odor producing compounds in the drinking water. Study shows that metal doping increases BET surface area, thus enhancing efficiency of titania to adsorb Geosmin and 2-MIB. The concentrations examined in this study are typically the levels that cause odor problems in lake water. Whilst activated carbon is still useful for off-flavours removal, metal doped titania nanoparticles are far more effective. Fe-TiO₂ showed 95% and 93% Geosmin and 2-MIB removal. Pt-TiO₂ was found to be most efficient; it removed 98% of Geosmin and 97% of 2-MIB as compared to 82% and 73% Geosmin and 2-MIB removal by most widely used granular activated carbon. Smaller size, extremely large surface area (567 m²/g), and more active adsorption site make Pt-TiO₂ as superior adsorbent. Further work is also being undertaken to refine the process for implementation in commercial applications.

Conflict of Interests

The authors declare that there is no conflict of interests regarding the publication of this paper.

Acknowledgment

The authors gratefully acknowledge financial support from the National University of Science and Technology, Islamabad, Pakistan.

References

- [1] M. Durrer, U. Zimmermann, and F. Jüttner, "Dissolved and particle-bound geosmin in a mesotrophic lake (Lake Zürich): spatial and seasonal distribution and the effect of grazers," *Water Research*, vol. 33, no. 17, pp. 3628–3636, 1999.
- [2] A. Peter and U. Von Gunten, "Oxidation kinetics of selected taste and odor compounds during ozonation of drinking water," *Environmental Science and Technology*, vol. 41, no. 2, pp. 626–631, 2007.
- [3] T.-F. Lin, J.-Y. Wong, and H.-P. Kao, "Correlation of musty odor and 2-MIB in two drinking water treatment plants in South Taiwan," *Science of the Total Environment*, vol. 289, no. 3, pp. 225–235, 2002.
- [4] I. H. Suffet, G. A. Burlingame, P. E. Rosenfeld, and A. Bruchet, "The value of an odor-quality-wheel classification scheme for wastewater treatment plants," *Water Science and Technology*, vol. 50, no. 9, pp. 25–32, 2004.
- [5] P. Westerhoff, M. Rodriguez-Hernandez, L. Baker, and M. Sommerfeld, "Seasonal occurrence and degradation of 2-methylisoborneol in water supply reservoirs," *Water Research*, vol. 39, no. 20, pp. 4899–4912, 2005.
- [6] D. Sun, J. Yu, W. An, M. Yang, G. Chen, and S. Zhang, "Identification of causative compounds and microorganisms for musty odor occurrence in the Huangpu River, China," *Journal of Environmental Sciences*, vol. 25, no. 3, pp. 460–465, 2013.
- [7] D. M. C. Rashash, A. M. Dietrich, and R. C. Hoehn, "Flavor profile analysis of selected odorous compounds," *The American Water Works Association*, vol. 89, no. 2, pp. 131–142, 1997.
- [8] S. B. Watson, M. Charlton, Y. R. Rao et al., "Off flavours in large waterbodies: physics, chemistry and biology in synchrony," *Water Science and Technology*, vol. 55, no. 5, pp. 1–8, 2007.
- [9] S.-W. Jung, K.-H. Baek, and M.-J. Yu, "Treatment of taste and odor material by oxidation adsorption," *Water Science and Technology*, vol. 49, no. 9, pp. 289–295, 2004.
- [10] L. Ho, G. Newcombe, and J.-P. Croué, "Influence of the character of NOM on the ozonation of MIB and geosmin," *Water Research*, vol. 36, no. 3, pp. 511–518, 2002.
- [11] S. L. N. Elhadi, P. M. Huck, and R. M. Slawson, "Removal of geosmin and 2-methylisoborneol by biological filtration," *Water Science and Technology*, vol. 49, no. 9, pp. 273–280, 2004.
- [12] C. Ng, J. N. Lasso, W. E. Marshall, and R. M. Rao, "Freundlich adsorption isotherms of agricultural by-product-based powdered activated carbons in a geosmin-water system," *Bioresource Technology*, vol. 85, no. 2, pp. 131–135, 2002.
- [13] M. Pirbazari, V. Ravindran, B. N. Badriyha, S. Craig, and M. J. McGuire, "GAC adsorber design protocol for the removal of off-flavors," *Water Research*, vol. 27, no. 7, pp. 1153–1166, 1993.
- [14] R. Srinivasan and G. A. Sorial, "Treatment of taste and odor causing compounds 2-methyl isoborneol and geosmin in drinking water: a critical review," *Journal of Environmental Sciences*, vol. 23, no. 1, pp. 1–13, 2011.
- [15] T. Balaji and H. Matsunaga, "Adsorption characteristics of As(III) and As(V) with titanium dioxide loaded Amberlite XAD-7 resin," *Analytical Sciences*, vol. 18, no. 12, pp. 1345–1349, 2002.
- [16] L. A. Lawton, P. K. J. Robertson, R. F. Robertson, and F. G. Bruce, "The destruction of 2-methylisoborneol and geosmin using titanium dioxide photocatalysis," *Applied Catalysis B: Environmental*, vol. 44, no. 1, pp. 9–13, 2003.
- [17] M. A. Behnajady, N. Modirshahla, M. Shokri, and B. Vahid, "Effect of operational parameters on degradation of malachite green by ultrasonic irradiation," *Ultrasonics Sonochemistry*, vol. 15, no. 6, pp. 1009–1014, 2008.
- [18] Y. Tang, Z. Jiang, Q. Tay et al., "Visible-light plasmonic photocatalyst anchored on titanate nanotubes: a novel nanohybrid with synergistic effects of adsorption and degradation," *RSC Advances*, vol. 2, no. 25, pp. 9406–9414, 2012.
- [19] Y. Tang, Z. Jiang, J. Deng et al., "Synthesis of nanostructured silver/silver halides on titanate surfaces and their visible-light photocatalytic performance," *ACS Applied Materials and Interfaces*, vol. 4, no. 1, pp. 438–446, 2012.
- [20] A. Bhatnagar, E. Kumar, and M. Sillanpää, "Nitrate removal from water by nano-alumina: characterization and sorption studies," *Chemical Engineering Journal*, vol. 163, no. 3, pp. 317–323, 2010.
- [21] L. Ho, D. Hoefel, F. Bock, C. P. Saint, and G. Newcombe, "Biodegradation rates of 2-methylisoborneol (MIB) and geosmin through sand filters and in bioreactors," *Chemosphere*, vol. 66, no. 11, pp. 2210–2218, 2007.
- [22] N. Saifuddin, C. Y. Nian, L. W. Zhan, and K. X. Ning, "Chitosan-silver nanoparticles composite as point-of-use drinking water filtration system for household to remove pesticides in water," *Asian Journal of Biochemistry*, vol. 6, no. 2, pp. 142–159, 2011.
- [23] S. R. Chowdhury and E. K. Yanful, "Arsenic and chromium removal by mixed magnetite-maghemite nanoparticles and the effect of phosphate on removal," *Journal of Environmental Management*, vol. 91, no. 11, pp. 2238–2247, 2010.
- [24] F. Deniz and S. Karaman, "Removal of an azo-metal complex textile dye from colored aqueous solutions using an agro-residue," *Microchemical Journal*, vol. 99, no. 2, pp. 296–302, 2011.
- [25] D. Cook and G. Newcombe, "Can we predict the removal of MIB and geosmin with PAC by using water quality parameters?" *Water Science and Technology: Water Supply*, vol. 4, no. 4, pp. 221–226, 2004.
- [26] W. T. Tsai, C. Y. Chang, C. H. Ing, and C. F. Chang, "Adsorption of acid dyes from aqueous solution on activated bleaching earth," *Journal of Colloid and Interface Science*, vol. 275, no. 1, pp. 72–78, 2004.



Hindawi

Submit your manuscripts at
<http://www.hindawi.com>

